

GenCepcion: Evaluate Vision LLMs with Unlabeled Unimodal Data

Lele Cao^{a,b,*}, Valentin Buchner^{b,c,*}, Zineb Senane^{b,d,e,f}, Fangkai Yang^d

^aMicrosoft Gaming (ABK), Stockholm, Sweden

^bEQT Group (Motherbrain), Stockholm, Sweden

^cChapter Two, Stockholm, Sweden

^dKTH Royal Institute of Technology, Stockholm, Sweden

^eTélécom Paris, Palaiseau, France

^fFever Energy, Stockholm, Sweden

Abstract

Multimodal Large Language Models (MLLMs) are typically assessed using expensive annotated multimodal benchmarks, which often lag behind the rapidly evolving demands of MLLM evaluation. This paper outlines and validates GenCepcion, a novel, annotation-free evaluation method that requires only unimodal data to measure inter-modality semantic coherence and inversely assesses MLLMs' tendency to hallucinate. This approach eliminates the need for costly data annotation, minimizes the risk of training data contamination, is expected to result in slower benchmark saturation, and avoids the illusion of emerging abilities. Inspired by the DrawCepcion game, GenCepcion begins with a non-textual sample and proceeds through iterative description and generation steps. The semantic drift across iterations is quantified using the GC@T metric. While GenCepcion is principally applicable to MLLMs across various modalities, this paper focuses on its implementation and validation for Vision LLMs (VLLMs). Based on the GenCepcion method, we establish the MMECepcion benchmark for evaluating VLLMs, and compare the performance of several popular VLLMs and human annotators. Our empirical results validate GenCepcion's effectiveness, demonstrating strong correlations with established VLLM benchmarks. VLLMs still significantly lag behind human performance and struggle especially with text-intensive tasks.

Keywords:

multimodal large language model, evaluation, benchmark

1. Introduction

Large Language Models (LLMs) demonstrate exceptional abilities in natural language understanding, reasoning, and problem-solving. Multimodal LLMs (MLLMs) enhance these capabilities by incorporating multiple modalities, with the visual modality being predominant and highly commercialized (Achiam et al., 2023; Liu et al., 2023b; Jiang et al., 2023; Ye et al., 2023). Building on LLMs, MLLMs integrate non-textual modalities, enabling richer interactions and broader applications in real-world scenarios. However, there is a lack of comprehensive evaluation methods to compare different MLLM architectures and training approaches (Fu et al., 2023).

In response, the community has developed several MLLM benchmarks, as detailed by Xu et al. (2022); Dai et al. (2023); Wang et al. (2023); Ye et al. (2023); Li et al. (2023c); Zhao et al. (2023). They primarily focus on the visual (i.e., image) and textual input modality due to that VLLMs (Vision LLMs)¹ are the most widely used and readily

*Equal contribution. Corresponding author: Lele Cao (lelecao@microsoft.com)

Source code and leaderboard: <https://github.com/llcresearch/GenCepcion>

This work was initiated during the author's tenure at EQT Motherbrain, with significant parts completed independently thereafter. It represents personal research conducted outside the scope of employment responsibilities. Relevant employers have been informed and have provided consent for publication.

¹Vision Large Language Models (VLLMs) are a specialized subclass of Multimodal Large Language Models (MLLMs) designed to integrate visual and textual modalities for tasks such as image captioning, visual question answering, and multimodal reasoning. While VLLMs are generally capable of processing various visual data types, their most common input is images, owing to the abundance of annotated image-text datasets and the maturity of image processing technologies.

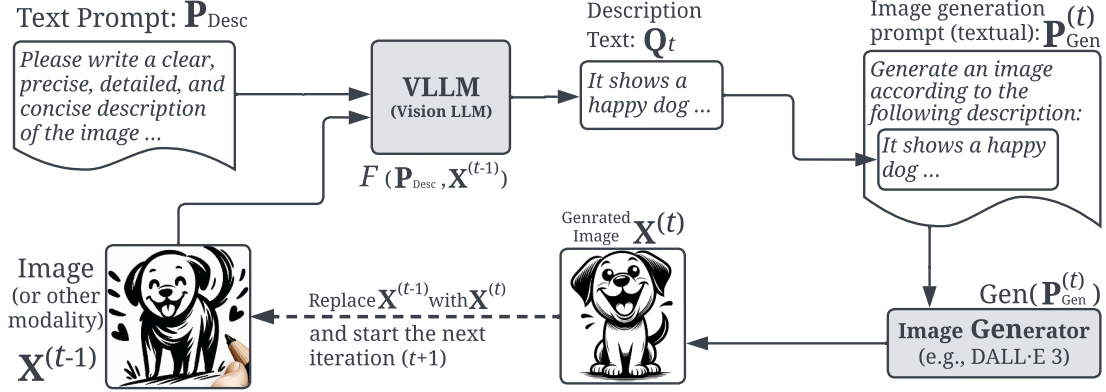


Figure 1: An illustration of the t -th iteration in the GenCepion evaluation procedure for VLLMs. Using the image modality as an example, the process begins with an existing image $\mathbf{X}^{(0)}$ sourced from a unimodal image dataset for the first iteration ($t=1$). The VLLM provides a detailed description of the image, which is then used by an image generator to produce $\mathbf{X}^{(t)}$.

available MLLMs on the market. However, these benchmarks face common challenges:

- (1) They predominantly rely on multimodal datasets that demand high-quality annotations, which is costly and restrictive in capturing the evolving capabilities of MLLMs (Fu et al., 2023). This has been shown to result in increasing speed in benchmark saturation while contemporary models still struggle on trivial real-world tasks (Kiela et al., 2021). Emerging methods like CrossCheckGPT (Sun et al., 2024), designed specifically for MLLM evaluation via cross-system consistency, provide a more relevant, annotation-free alternative. On a broader scope, methods like PRD (Li et al., 2023b) focus on LLM evaluation through peer-based rankings and may be further adapted for MLLM evaluation tasks.
- (2) MLLM evaluation benchmarks that rely on discrete metrics like accuracy may falsely suggest emergent abilities and do not allow predictable projections of performance improvements from model scaling (Schaeffer et al., 2023).
- (3) The evaluation scores may not reflect true performance on real-world tasks due to potential contamination of MLLM training data by benchmark datasets, as reported for LLM pretraining corpora (Dodge et al., 2021; Yang et al., 2023).
- (4) The content of one modality is often not needed to answer benchmark questions, as the answer can often be inferred from the question or the MLLM’s pretraining knowledge.

As a consequence of both (3) and (4), some MLLMs can excel on vision QA benchmarks without even being provided the image that is associated with the question. Existing solutions either only tackle a subset of these challenges, or focus on specific tasks such as image captioning (Lee et al., 2024).

We propose GenCepion to address all highlighted challenges involved in the evaluation of task-agnostic MLLMs. GenCepion is designed to be a general evaluation framework that can be applied across modalities. To validate its effectiveness, this paper focuses on Vision LLMs (VLLMs), leveraging the visual modality as an illustrative example. GenCepion addresses challenge (1) by relying on easily accessible unimodal datasets, which allows for cost-effective and scalable benchmark creation. Relying on unimodal datasets additionally addresses challenge (3) and (4), as it allows to easily use previously unseen datasets for MLLM evaluation, and enforces the relevance of the provided modality for excelling at this task. To tackle challenge (2), GenCepion uses the continuous $\text{GC}@T$ metric, providing a more nuanced evaluation compared to discrete metrics, allowing for better projections of performance improvements and avoiding the mirage of emergent abilities.

On a high and general level, GenCepion assesses MLLMs’ ability to consistently maintain semantic coherence across modalities by iteratively generating and describing non-textual samples and measures the continuous $\text{GC}@T$ metric. This approach simultaneously evaluates the MLLM’s tendency to hallucinate, as this inversely correlates with semantic coherence. Further, an MLLM’s ability to provide complete yet concise descriptions of non-textual samples measures a diverse range of specialized abilities. For instance, to perform well at describing an image using a limited

number of tokens, it is advantageous to be able to reason over people’s emotions and intentions behind their actions, infer the current and preceding weather, count objects, and recognize artistic styles. This list can be extended to various abilities depending on the non-textual modality and the content of the samples used during the GenCepcion process. The main contributions of this paper are the following:

- Proposing GenCepcion, an evaluation method that principally allows for using unlabeled unimodal datasets for MLLM evaluation.
- Introducing *MMEception*, a Vision LLM (VLLM) evaluation benchmark utilizing the GenCepcion method. *MMEception* uses the images from the MME benchmark (Fu et al., 2023), but without their annotated question and answer pairs.
- Evaluating seven leading VLLMs on the *MMEception* benchmark and comparing results with other popular VLLM benchmarks and human performance.

We will elaborate on the proposed implementation of the GenCepcion method, detail our experimental setup, and discuss our findings.

2. GenCepcion

Our approach, GenCepcion, is inspired by a multi-player game DrawCepcion² (a.k.a., Scrawl or Whispany). In this game, the first player is given an image and describes it verbally to the next player. This player then attempts to recreate the image based on the description. The cycle repeats, often resulting in amusing deviations from the original image. The challenge and objective are to maintain the initial information through iterative transitions between verbal descriptions and drawings. Similarly, a proficient Multimodal Language Model (MLLM), which models multiple modalities such as text and images, should excel at this task. Recognizing that MLLMs can encompass modalities beyond just visual cues, such as audio and graphs, we name our approach GenCepcion, covering a broader scope than the visually-centric DrawCepcion. For the sake of clarity and alignment with our experiments, we will focus on VLLMs in the remainder of this section to walk through the GenCepcion approach.

While it may not be possible to preserve the initial information perfectly due to varying levels of richness, accuracy, and ambiguity in different modalities, a more capable MLLM will minimize the semantic drift from the original input. This contrasts with common benchmarks that aim for complete saturation, highlighting a key advantage of the GenCepcion framework: the creation of benchmarks that are more challenging to saturate. With complex initial samples, such as images of real-world scenes or graphs with numerous nodes and edges, this may even result in impossible-to-saturate benchmarks. Aiming for minimum rather than no semantic drift, this would allow to rank MLLMs relative to each other while continuously leaving space for more performant models.

2.1. Procedure

Unlike existing MLLM benchmarks (often focused on VLLMs) that rely on multimodal samples, GenCepcion is designed to operate on unimodal datasets, significantly streamlining dataset acquisition efforts. For illustrative purposes, we employ the image modality as a representative non-textual modality throughout this exposition. Let us consider an image dataset \mathcal{D} comprising images $\mathbf{X}_1, \mathbf{X}_2, \dots, \mathbf{X}_N$, similar to well-established datasets like ImageNet (Deng et al., 2009), CIFAR (Krizhevsky et al., 2009), and STL (Coates et al., 2011). Without loss of generality, any image from \mathcal{D} is denoted as \mathbf{X} .

GenCepcion operates iteratively, from $t = 1$ to a pre-defined maximum iteration $t = T$. Each iteration, as depicted in Figure 1, begins with an image $\mathbf{X}^{(t-1)}$ and yields a new image $\mathbf{X}^{(t)}$. The first iteration ($t = 1$) starts with the original image $\mathbf{X}^{(0)}$ from \mathcal{D} . During any given iteration t , the VLLM receives a textual prompt \mathbf{P}_{Desc} (Table 1), instructing the VLLM to generate a comprehensive description \mathbf{Q}_t for the input image $\mathbf{X}^{(t-1)}$:

$$\mathbf{Q}_t := F(\mathbf{P}_{\text{Desc}}, \mathbf{X}^{(t-1)}), \text{ where } F \text{ denotes the generation function of any VLLMs.} \quad (1)$$

²<https://wikipedia.org/wiki/drawception>

Please write a clear, precise, detailed, and concise description of all elements in the image. Focus on accurately depicting various aspects, including but not limited to the colors, shapes, positions, styles, texts and the relationships between different objects and subjects in the image. Your description *should be thorough enough to guide a professional in recreating this image solely based on your textual representation*. Remember, only include descriptive texts that directly pertain to the contents of the image. You must complete the description using less than 500 words.

Table 1: The fixed textual prompt \mathbf{P}_{Desc} instructs the MLLM to produce a description of the input $\mathbf{X}^{(t-1)}$.

Following this, an image generation prompt $\mathbf{P}_{\text{Gen}}^{(t)}$ is constructed as “Generate an image that fully and precisely reflects this description: $\langle \mathbf{Q}_t \rangle$ ”. This prompt guides a pretrained image generation model, such as DALL·E (Ramesh et al., 2021) or Imagen (DeepMind, 2023), to create a new image, $\mathbf{X}^{(t)}$:

$$\mathbf{X}^{(t)} := \text{Gen}(\mathbf{P}_{\text{Gen}}^{(t)}), \quad (2)$$

where $\text{Gen}(\cdot)$ signifies the chosen image generator. Each subsequent iteration $t + 1$ starts with the image $\mathbf{X}^{(t)}$ generated in the previous iteration. Upon completing all iterations, we obtain a series of $T + 1$ images: $\mathbf{X}^{(0)}, \mathbf{X}^{(1)}, \dots, \mathbf{X}^{(T)}$, with the initial image being the original and the rest sequentially produced across the iterations.

The textual prompt \mathbf{P}_{Desc} is intentionally kept short and concise to minimize potential variations in model behaviours due to susceptibility to prompt composition (Loya et al., 2023).

2.2. Metric: GC@T

Our primary objective is to measure the semantic divergence of each generated image $\mathbf{X}^{(t)}$ (for $t \in \{1, 2, \dots, T\}$) from the original image $\mathbf{X}^{(0)}$. We use a pretrained image encoder, such as ViT (Dosovitskiy et al., 2021), to transform all images, resulting in $T + 1$ image embeddings denoted as $\mathbf{z}^{(0)}, \mathbf{z}^{(1)}, \dots, \mathbf{z}^{(T)}$, where $\mathbf{z}^{(t)} := \text{Enc}(\mathbf{X}^{(t)})$. We then compute the cosine similarity between $\mathbf{z}^{(0)}$ and each $\mathbf{z}^{(t)}$ (for $t \in \{1, 2, \dots, T\}$), yielding T similarity scores: $s^{(1)}, s^{(2)}, \dots, s^{(T)}$. Here, $s^{(t)} \in [-1.0, 1.0]$ approximates the level of semantic drift in the t -th iteration of the GenCception procedure. To quantify the overall speed and magnitude of semantic drift, we calculate the GenCception score over T iterations, denoted as $\text{GC}@T \in [-1.0, 1.0]$, as follows:

$$\text{GC}@T := \frac{\sum_{t=1}^T (t \cdot s^{(t)})}{\sum_{t=1}^T t}. \quad (3)$$

This is a normalized and continuous metric that weights later iterations more heavily for two reasons: (1) similar to the DrawCception game, the last image’s deviation from the initial image is most telling; (2) we aim to capture performance and dynamics across the entire iterative sequence. A high $\text{GC}@T$ value signifies an exceptional ability to maintain inter-modal (text-image) semantic congruence, effectively curbing the propensity for rapid or extensive deviation from the semantics encapsulated in the original image. Notably, $\text{GC}@1$ is equivalent to $s^{(1)}$. For the pseudo code detailing the GenCception procedure and the calculation of the average $\text{GC}@T$ metric over the entire dataset \mathcal{D} , see Algorithm 1.

For the special case of VLLMs that are evaluated in this study, we additionally replace using ViT embeddings and cosine similarity with the Frechet Inception Distance (FID), a metric commonly used to evaluate image generation models (Heusel et al., 2017). The FID is calculated between the original dataset of images $\mathcal{D}^{(0)}$, and the images generated from the respective dataset using the GenCception process $\mathcal{D}^{(t)}$, yielding T FID scores: $\text{fid}^{(1)}, \text{fid}^{(2)}, \dots, \text{fid}^{(T)}$. The $\text{GC}_{\text{FID}}@T$ score is then calculated as:

$$\text{GC}_{\text{FID}}@T := \frac{\sum_{t=1}^T (t \cdot \text{fid}^{(t)})}{\sum_{t=1}^T t}. \quad (4)$$

As the FID indicates a distance rather than a similarity between two sets of images, a lower distance indicates better performance, and consequently a lower $\text{GC}_{\text{FID}}@T$ score indicates a more capable VLLM.

Algorithm 1: Calculate $GC@T$ via GenCception for a specific VLLM under evaluation

Input: VLLM to be evaluated, a unimodal dataset \mathcal{D} : $\mathbf{X}_1^{(0)}, \dots, \mathbf{X}_n^{(0)}, \dots, \mathbf{X}_N^{(0)}$, fixed textual prompt \mathbf{P}_{Desc} , a sample generator $\text{Gen}(\cdot)$, and a sample encoder $\text{Enc}(\cdot)$

Output: Average $GC@T$ metric over \mathcal{D}

Parameter: The number of iterations T

```
1:  $GC@T = 0$ 
2: for ( $n = 1; n \leq N; n++$ ) do
3:    $\mathbf{z}^{(0)} := \text{Enc}(\mathbf{X}_n^{(0)})$ ;
4:   for ( $t = 1; t \leq T; t++$ ) do
5:     Generate description  $\mathbf{Q}_t$  for  $\mathbf{X}_n^{(t-1)}$  using (1);
6:     Create  $\mathbf{P}_{\text{Gen}}^{(t)}$  using  $\mathbf{Q}_t$ ;
7:     Generate  $\mathbf{X}_n^{(t)}$  according to (2);
8:      $s^{(t)} := \text{CosineSimilarity}(\mathbf{z}^{(0)}, \text{Enc}(\mathbf{X}_n^{(t)}))$ ;
9:   end
10:  Calculate  $GC@T += \sum_{t=1}^T (t \cdot s^{(t)}) / \sum_{t=1}^T t$ ; (3)
11: end
12: return  $GC@T / N$ ;
```

3. Experiments

We run several extensive experiments to validate the GenCception method by comparing the $GC@T$ scores achieved by several VLLMs to the scores they achieve on carefully crafted established benchmarks and to average human performance. Although GenCception’s design merely requires unimodal image datasets, we employ the same data as used by a recent and well-validated MLLM benchmark, MME (Fu et al., 2023). While we discard the annotated question-answer pairs associated with the images in this benchmark, this provides us with the ability (1) to facilitate direct comparison with metrics that include textual QA (question-answering) annotations, and (2) to enable a detailed assessment of MLLM performance across MME’s 14 meticulously crafted sample categories. Attributing this newly created benchmark to the MME dataset and the GenCception method, we refer to it as the *MMECception* benchmark.

We select seven VLLMs – Gemini1.5-Pro (Reid et al., 2024), GPT-4o (OpenAI, 2024), GPT-4V (Achiam et al., 2023), Claude3-Opus (Anthropic, 2023), LLaVA-7B/13B (Liu et al., 2023b) and mPLUG-Owl2 (Ye et al., 2023) – based on their superior performance on the OpenCompass multimodal leaderboard (OpenCompass, 2023), which incorporates a comprehensive set of benchmarks like MME (Fu et al., 2023), HallusionBench (Liu et al., 2023a), MMStar (Chen et al., 2024), SeedBench (Li et al., 2023a), and AI2D (Kembhavi et al., 2016). We use DALL-E as the default image generation model. To prevent potential bias towards OpenAI-developed VLLMs, which might have had access to DALL-E-generated images during their training, we perform an additional evaluation of all VLLMs on the $GC@1$ score using Imagen2 as an image generation model. We set the temperature parameter to 0 in both the VLLMs and image generators to minimize the stochasticity in model outputs.

As humans are well versed at integrating vision and language modalities, we aim to quantify average human performance on the *MMECception* benchmark. As the GenCception procedure is a labor-intensive and time-consuming task for humans, we randomly select 5 images from each MME category, and by providing human annotators with the same prompts as defined in Table 1, collect results and calculate the $GC@1$ metric. Five human annotators (3 master students, 1 lecturer, and 1 artist) were recruited to describe one image of each category such that each image in a category is described by a different person to mitigate personal performance differences. The annotators were given 14 weeks to perform this task and were awarded a generous reimbursement of €40 each to ensure sufficient dedication. All annotators were either native English speakers or fluent at a professional level.

3.1. Quantitative results

We partition the 14 MME categories into two groups based on content type: visual-intensive (10 categories: *existence*, *count*, *position*, *color*, *poster*, *celebrity*, *scene*, *landmark*, *artwork*, and *commonsense reasoning*) and textual-intensive (4 categories: *code reasoning*, *numerical calculation*, *text translation*, and *OCR*). $GC@3$ scores on the

Sample group & category	Gemini1.5-Pro			Claude3-Opus			GPT-4o			GPT-4V			mPLUG-Owl2			LLaVA-1.3B			LLaVA-7B			
	MME↑	GC@3↑	GC@3↓	MME↑	GC@3↑	GC@3↓	MME↑	GC@3↑	GC@3↓	MME↑	GC@3↑	GC@3↓	MME↑	GC@3↑	GC@3↓	MME↑	GC@3↑	GC@3↓	MME↑	GC@3↑	GC@3↓	
	ΣACC	Cosine	FID	ΣACC	Cosine	FID	ΣACC	Cosine	FID	ΣACC	Cosine	FID	ΣACC	Cosine	FID	ΣACC	Cosine	FID	ΣACC	Cosine	FID	
visual-intensive samples	Existence	190.0	0.437	269.8	183.3	0.382	273.7	195.0	0.400	266.5	175.0	0.422	265.1	185.0	0.323	296.9	195.0	0.305	322.0	195.0	0.308	318.1
	Count	148.3	0.389	272.6	116.7	0.348	285.3	190.0	0.388	277.5	153.3	0.404	277.4	160.0	0.299	316.1	165.0	0.294	319.7	148.3	0.253	326.1
	Position	105.0	0.357	253.7	76.7	0.357	266.1	145.0	0.398	260.6	85.0	0.408	253.3	75.0	0.306	294.0	135.0	0.255	298.9	123.3	0.285	286.0
	Color	175.0	0.474	234.8	118.3	0.385	267.6	180.0	0.421	246.1	141.7	0.403	243.7	138.3	0.290	310.1	165.0	0.300	305.6	170.0	0.284	304.5
	Poster	175.2	0.374	206.0	149.7	0.360	206.0	192.2	0.335	203.7	187.8	0.324	209.4	154.8	0.243	209.2	163.6	0.215	240.9	154.1	0.214	244.3
	Celebrity	169.4	0.362	191.0	77.6	0.317	192.5	46.8	0.331	193.3	53.5	0.332	189.1	167.9	0.232	211.3	144.4	0.206	223.7	153.2	0.188	233.6
	Scene	147.0	0.423	173.7	149.8	0.374	174.7	148.5	0.401	171.5	141.2	0.393	173.7	157.8	0.299	194.4	162.8	0.277	198.0	160.8	0.266	196.3
	Landmark	176.8	0.375	182.1	113.0	0.344	188.9	175.5	0.372	182.0	104.0	0.353	182.6	158.8	0.275	206.0	150.8	0.242	224.3	154.8	0.252	214.4
	Artwork	152.2	0.412	171.1	136.8	0.385	170.4	144.0	0.415	169.2	115.0	0.421	170.3	136.0	0.252	202.2	98.8	0.212	213.3	110.0	0.210	215.3
	Commonsense	150.0	0.464	216.5	115.0	0.432	210.4	174.3	0.448	213.9	155.0	0.471	208.1	127.9	0.353	237.2	115.7	0.334	248.9	117.1	0.294	254.4
textual-intensive	Visual Mean	158.9	0.407	217.1	123.7	0.368	223.6	159.1	0.391	218.4	131.2	0.393	217.3	146.2	0.287	247.7	149.7	0.264	259.5	148.7	0.255	259.3
	Visual Rank	2	1	1	7	4	4	1	3	3	6	2	2	5	5	5	3	6	7	5	7	6
	Code reasoning	117.5	0.213	310.0	70.0	0.245	267.4	182.5	0.255	299.7	147.5	0.193	302.9	65.0	0.176	327.6	55.0	0.144	323.5	50.0	0.107	398.2
	Numerical calc.	110.0	0.268	346.5	67.5	0.229	349.3	170.0	0.282	346.4	80.0	0.240	322.5	45.0	0.192	362.0	35.0	0.195	367.4	50.0	0.455	366.0
	Text translation	162.5	0.240	334.6	45.0	0.236	362.5	192.5	0.211	326.9	55.0	0.157	368.0	112.5	0.081	365.2	85.0	0.116	352.3	65.0	0.111	424.4
	OCR	170.0	0.367	233.2	167.5	0.362	245.5	192.5	0.362	246.2	177.5	0.393	238.0	102.5	0.276	255.4	95.0	0.239	270.6	65.0	0.222	283.7
	Textual Mean	140.0	0.272	306.1	87.5	0.268	306.2	184.4	0.278	304.8	115.0	0.246	307.9	81.3	0.181	327.6	67.5	0.174	328.5	57.5	0.149	368.1
	Textual Rank	2	2	2	4	3	3	1	1	1	3	4	4	5	5	5	6	6	6	7	7	7
	Overall Mean	153.5	0.368	242.5	113.3	0.340	247.2	166.3	0.359	243.1	126.5	0.351	243.2	127.6	0.257	270.5	126.1	0.238	279.2	122.6	0.225	290.1
	Overall Rank	2	1	1	7	4	4	1	2	2	4	3	3	3	5	5	5	6	6	6	6	7
HallusionBench*	45.2 (rank=3)			37.8 (rank=4)			51.7 (rank=1)			46.5 (rank=2)			25.7 (rank=6)			24.5 (rank=7)			27.6 (rank=5)			
	MMStar*			38.6 (rank=5)			45.7 (rank=3)			61.6 (rank=1)			47.7 (rank=2)			34.8 (rank=6)			40.1 (rank=4)			
	SEEDBench (Test)*			70.7 (rank=3)			64.0 (rank=7)			76.4 (rank=1)			71.6 (rank=2)			64.5 (rank=6)			67.9 (rank=4)			
	AI2D*			70.2 (rank=4)			70.6 (rank=3)			82.2 (rank=1)			75.5 (rank=2)			55.7 (rank=7)			61.3 (rank=5)			
	OpenCompass*			62.7 (rank=3)			57.7 (rank=4)			66.3 (rank=1)			63.3 (rank=2)			46.3 (rank=7)			48.8 (rank=5)			

* Results are sourced from https://huggingface.co/spaces/opencompass/open_vlm_leaderboard as of 2024-04-25 (except GPT-4o) and 2024-05-23 (for GPT-4o).

↓ Results are obtained using FID to measure the similarity between images. <https://github.com/GaParmar/clean-fid>

Table 2: Evaluation results of GC@3, MME, HallusionBench and OpenCompass on visual(Vis)-intensive and textual(Text)-intensive images. Best results per metric and category (over different MLLMs) are **bolded**.

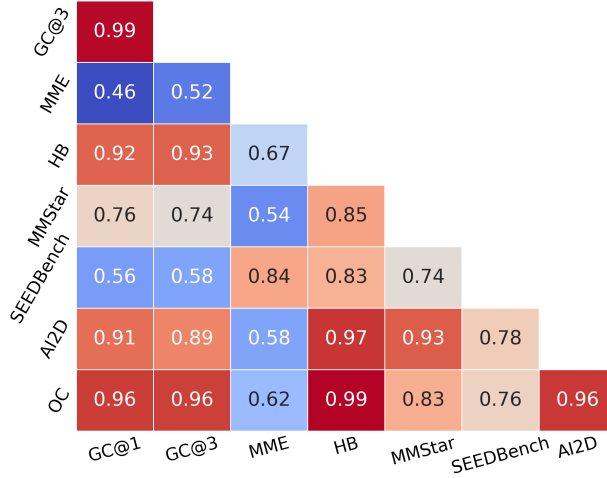


Figure 2: Correlation Matrix of GC@1 and GC@3 scores on *MMEception*, and several other benchmarks.

MMEception benchmark and accuracy on the original MME benchmark are reported per category and as aggregations in Table 2. Additionally, we include the scores and ranks of all evaluated VLLMs on the OpenCompass (OpenCompass, 2023), MME (Fu et al., 2023), HallusionBench (Liu et al., 2023a), MMStar (Chen et al., 2024), SeedBench (Li et al., 2023a), and AI2D (Kembhavi et al., 2016) leaderboards. Notably, Gemini1.5-Pro leads our rankings, followed by GPT-4o, GPT-4v, Claude3-Opus, mPLUG-Owl2, and LLaVA-13B/7B. The GenCepion method shows robustness to the similarity metric used, as the overall ranking remains identical when using cosine similarity or FID distance for calculating GC@T scores.

	GC@1	GC@3	MME	HallusionBench
GC@1 (essentially the same as $s^{(1)}$)	-	0.99	0.46	0.92
GC@3	0.99	-	0.52	0.93
$s^{(3)}$ (GC@3 without weighting by t)	0.98	0.99	0.46	0.94
CrossCheckGPT (Image-to-text)	0.96	0.94	0.42	0.97

Table 3: Correlation matrix comparing GC@1, GC@3, $s^{(3)}$ (GC@3 without temporal weighting), and CrossCheckGPT with established benchmarks MME and HallusionBench.

Figure 2 presents a correlation matrix among GC@T scores and the benchmarks mentioned above, where the overall GC@T scores are averaged over the GC@T scores of all MME categories. The strong correlations with the OpenCompass scores incorporating the results of multiple meticulously crafted benchmarks indicate that *MMEception* provides a comprehensive evaluation that may complement existing benchmarks. Further, GenCepion appears to effectively measure a VLLM’s tendency to hallucinate, as demonstrated by the strong correlations with HallusionBench. While these observations are further emphasized by the correlations with MMStar and AI2D, the only moderate correlations with MME and SEEDBench provide more nuanced insights. As MME displays these moderate correlations also with the other benchmarks, it can be reasoned that it measures dimensions supplement to those measured by other benchmarks and GenCepion. SEEDBench on the other hand correlates strongly with other benchmarks, but only moderately with GC@T scores. This indicates that SEEDBench measures aspects that are also measured by other benchmarks, but fail to be captured by GenCepion. Future research could focus on identifying these aspects to potentially incorporate them into GenCepion.

One of the key strengths of GenCepion lies in its annotation-free evaluation methodology, a concept also reflected in emerging evaluation methods such as CrossCheckGPT Sun et al. (2024). CrossCheckGPT ranks hallucinations by evaluating the consistency of outputs across independent MLLM models. In 3, we analyze the correlation of CrossCheckGPT with GenCepion, MME, and HallusionBench scores. The results show strong correlations between CrossCheckGPT and both GenCepion and HallusionBench, affirming its capability to capture key evaluative met-

Sample group & category		Gemini1.5-Pro		Claude3-Opus		GPT-4o		GPT-4V		mPLUG-Owl2		LLaVA-13B		LLaVA-7B	
		Dalle3	Imgn2	Dalle3	Imgn2	Dalle3	Imgn2	Dalle3	Imgn2	Dalle3	Imgn2	Dalle3	Imgn2	Dalle3	Imgn2
visual-intensive samples	Existence	0.505	0.529	0.500	0.532	0.536	0.521	0.505	0.530	0.427	0.515	0.416	0.485	0.418	0.506
	Count	0.456	0.489	0.466	0.490	0.456	0.494	0.498	0.506	0.378	0.463	0.408	0.466	0.341	0.416
	Position	0.511	0.491	0.495	0.480	0.469	0.460	0.501	0.473	0.346	0.452	0.359	0.454	0.350	0.402
	Color	0.545	0.525	0.489	0.501	0.480	0.473	0.506	0.490	0.345	0.471	0.420	0.457	0.318	0.436
	Poster	0.455	0.388	0.450	0.381	0.445	0.383	0.444	0.365	0.338	0.357	0.303	0.312	0.305	0.266
	Celebrity	0.417	0.384	0.424	0.382	0.418	0.373	0.433	0.389	0.319	0.336	0.284	0.317	0.263	0.313
	Scene	0.511	0.490	0.504	0.478	0.482	0.474	0.497	0.474	0.385	0.417	0.355	0.404	0.350	0.392
	Landmark	0.500	0.485	0.460	0.492	0.494	0.479	0.458	0.480	0.363	0.351	0.376	0.357	0.334	0.333
	Artwork	0.494	0.454	0.508	0.461	0.500	0.455	0.504	0.455	0.333	0.385	0.308	0.333	0.294	0.304
	Common.	0.545	0.531	0.535	0.507	0.562	0.526	0.563	0.535	0.425	0.493	0.429	0.473	0.417	0.458
	Vis Mean	0.494	0.477	0.483	0.470	0.484	0.464	0.491	0.470	0.366	0.424	0.366	0.406	0.339	0.383
	Vis Rank	1	1	4	2	3	4	2	2	5	5	5	6	7	7
textual-intensive	Code	0.364	0.177	0.304	0.180	0.395	0.179	0.333	0.263	0.281	0.100	0.260	0.168	0.186	0.108
	Numerical	0.322	0.417	0.333	0.389	0.366	0.456	0.325	0.383	0.322	0.225	0.336	0.265	0.259	0.222
	Text trans.	0.396	0.227	0.356	0.258	0.444	0.277	0.359	0.238	0.173	0.052	0.200	0.118	0.212	0.073
	OCR	0.462	0.500	0.486	0.448	0.421	0.441	0.482	0.417	0.358	0.384	0.368	0.385	0.351	0.320
	Text Mean	0.386	0.330	0.370	0.319	0.407	0.338	0.375	0.325	0.284	0.190	0.291	0.234	0.252	0.181
	Text Rank	2	2	4	4	1	1	3	3	6	6	5	5	7	7
Overall Mean		0.463	0.435	0.451	0.427	0.462	0.428	0.458	0.428	0.343	0.357	0.344	0.357	0.314	0.325
Overall Rank		1	1	4	4	2	2	3	2	6	5	5	5	7	7

Table 4: The impact of different image encoders, DALL-E 3 (Dalle3) vs. Imagen 2 (Imgn2), on GC@1 score. Best results per configuration and category (over different VLLMs) are **bolded**.

Sample group & category		Gemini1.5-Pro	Claude3-Opus	GPT-4o	GPT-4V	mPLUG-Owl2	LLaVA-13B	LLaVA-7B	Human	$\Delta\%$ between human & best
visual-intensive samples	Existence	<u>0.5841</u>	0.4563	0.5578	0.5434	0.3967	0.3524	0.3782	0.6402	+ 9.6045%
	Count	0.4140	0.3799	0.2725	<u>0.4882</u>	0.2364	0.3535	0.2038	0.5476	+ 12.1671%
	Position	0.5546	0.4959	0.4086	<u>0.5639</u>	0.3527	0.4285	0.3899	0.6409	+ 13.6549%
	Color	<u>0.7081</u>	0.6206	0.6139	0.5516	0.4047	0.4314	0.3506	0.8380	+ 18.3449%
	Poster	<u>0.5046</u>	0.4362	0.4939	0.4681	0.3998	0.3208	0.2905	0.5456	+ 8.1252%
	Celebrity	0.4182	0.3988	0.4369	<u>0.4447</u>	0.3714	0.2545	0.2160	0.4671	+ 5.0371%
	Scene	<u>0.6080</u>	0.5828	0.5229	0.5919	0.4842	0.3906	0.4057	0.6236	+ 2.5658%
	Landmark	0.4903	0.4932	0.5236	<u>0.5702</u>	0.3613	0.4174	0.3845	0.6045	+ 6.0154%
	Artwork	0.3725	<u>0.5304</u>	0.5297	0.5252	0.2938	0.2924	0.2336	0.5421	+ 2.2059%
	Commonsense	0.4338	<u>0.5375</u>	0.5047	0.4012	0.3244	0.4153	0.3532	0.6417	+ 19.3860%
Visual Mean		<u>0.5088</u>	0.4932	0.4865	0.5148	0.3625	0.3657	0.3206	0.6091	+ 9.7107%
text-intensive	Code reasoning	0.3689	<u>0.4085</u>	0.4043	0.3690	0.2923	0.2963	0.1975	0.5376	+ 31.6034%
	Numerical calc.	0.3652	0.3958	0.3940	0.4241	0.3474	<u>0.4409</u>	0.3423	0.5160	+ 17.0333%
	Text translation	<u>0.4480</u>	0.3949	0.4333	0.3803	0.0931	0.2372	0.1981	0.6196	+ 38.3036%
	OCR	0.4382	0.4329	0.3334	<u>0.4455</u>	0.2663	0.3371	0.2912	0.4696	+ 5.4097%
	Textual Mean	0.4051	<u>0.4080</u>	0.3913	0.4047	0.2498	0.3279	0.2573	0.5357	+ 23.0875%
Overall Mean		0.4792	0.4688	0.4593	<u>0.4834</u>	0.3303	0.3549	0.3025	0.5882	+ 13.5327%

Table 5: The performance of VLLMs and humans on the GC@1 metric, evaluated using 5 randomly drawn images per sample/image category. The best performance achieved by a VLLM is underlined.

rics. Notably, CrossCheckGPT exhibits a weaker correlation with MME, which is likely because the GenCception benchmark is developed using MME image samples, making it inherently more aligned with the MME framework.

GC@ T scores, as defined in Equation (3), are weighted by a temporal factor t . To examine the impact of this

weighting, we conducted an ablation study where the weighting mechanism was removed, effectively transforming $GC@T$ into $s^{(T)}$. Table 3 demonstrates that $s^{(3)}$ retains a high correlation with $GC@3$, yet its correlation with MME diminishes compared to the weighted version, while its alignment with HallusionBench remains consistent. Furthermore, unweighted scores correlate with MME in a uniform manner across different iterations, whereas the weighted scores show a progressive increase in correlation with MME as more iterations are applied. This indicates that temporal weighting amplifies later iterations’ influence, emphasizing cumulative semantic shifts captured by MME’s iterative design. Generally, stronger correlation with MME is desirable as it validates the alignment between GenCep-
tion’s metrics and an established benchmark, reinforcing GenCep-
tion’s ability to assess iterative semantic coherence effectively and reliably.

Table 4 compares $GC@1$ scores using different image generators, OpenAI’s DALL-E 3 (Ramesh et al., 2021) and Google DeepMind’s Imagen2 (DeepMind, 2023). Independent of image generator used, the rankings remain unchanged, except that on visual-intensive samples only, Claude3-Opus scores equally with GPT-4V. This provides evidence that even though DALL-E 3, GPT-4o, and GPT-4V were developed and trained by OpenAI, neither of OpenAI’s models has an advantage over non-OpenAI VLLMs.

Table 5 shows human performance on a subset of 5 randomly drawn images per category compared to the VLLM performance on the same subset of samples. It can be observed that humans outperform all VLLMs, with especially strong differences in performance for the text-intensive categories. The worst performance, relative to humans, is achieved on the *code reasoning* and *text translation* categories, the former containing images of code snippets and the latter of phrases written in simplified Chinese characters. The relatively best performance by VLLMs is achieved on the *scene* and *artwork* categories, which contain every-day life photos and popular artworks. This demonstrates that there is still substantial space for performance improvement, and that compared to humans, VLLMs still lack relevant competences. It must be noted that human performance here does not constitute an upper bound in possible scores to achieve, and that future generations of VLLMs may well outperform humans.

3.2. Qualitative Results

We qualitatively inspect our results by visualizing generated images together with their cosine similarity and $GC@T$ scores for two seed images across different categories, as shown in Figure 3. This visualization highlights the correlation between these scores and the visual characteristics of the images relative to the seed image. A key observation is that later iterations show an increased tendency to produce imagery deviating from the seed image, as indicated by lower $GC@T$ scores. This serves as an additional qualitative validation of the GenCep-
tion method and the *MMECep-
tion* benchmark, as using VLLMs scoring higher on the *MMECep-
tion* benchmark results in generated images that preserve more information from the seed image. For a wider range of examples across MME image categories and corresponding descriptions from each evaluated VLLM, readers are referred to Appendix A.

4. Discussion and Future Directions

This study validates the GenCep-
tion method with a focus on the visual modality primarily because (1) VLLMs are the most widely used and readily available MLLMs on the market, and (2) image generation and embedding tools have reached a mature and highly commercialized stage compared to other modalities. However, GenCep-
tion is designed to be modality-agnostic. The same iterative procedure (i.e., describing a unimodal sample and then re-generating it from the description) can, in principle, be applied to other non-text modalities like audio and video. The requirement is that (1) a generation model exists for the given modality, and (2) there is a suitable encoder to quantify the similarity between the original sample and the regenerated one. Moreover, recent advancements have introduced multimodal LLMs capable of both generating and interpreting multiple modalities simultaneously, such as Show-o (Xie et al., 2024), Emu3 (Wang et al., 2024), and JanusPro (Chen et al., 2025). In these cases, GenCep-
tion could leverage the same MLLM for both description and generation tasks, serving as a particularly valuable approach for directly measuring modality consistency within such unified multimodal systems.

Future research is invited to adapt GenCep-
tion to other non-text modalities, such as audio, video, and graphs. For instance, the framework can be initiated with a dataset of audio samples, and MLLMs can iteratively generate and describe the audio content. Similarly, for video and graph data, the process can involve generating textual descriptions of short video clips or graph structures and their recreation. While the core iterative process of GenCep-
tion remains applicable, these extensions require careful exploration of modality-specific generation and embedding models.



Figure 3: Demonstration of GenCception evaluation procedure: the images generated over 3 GenCception iterations for several MLLMs. The similarity $s^{(t)}$ scores (to the seed image) are shown on the top of images; GC@1 and GC@3 scores are printed on the bottom of the first and third image, respectively.

The broad skill assessment provided by GenCception goes along with the limitation that it is difficult to assess which skills contribute most to a high GC@ T score. Our analysis indicates that contemporary VLLMs perform poorly on text-intensive tasks while excelling in describing scenes and artworks. Future research could investigate this in a more fine-grained manner by creating datasets requiring specialized skills. For example, datasets could include images of complex emotions, dynamic movements, mechanical processes, or user interfaces. Additionally, combining GenCception with specifically designed similarity metrics may offer more detailed insights into specific MLLM abilities.

5. Conclusion

In this paper, we introduce GenCception to enhance the evaluation of rapidly evolving Multimodal Language Models (MLLMs). The GenCception method attempts to address key limitations of existing MLLM benchmarks, such as costly data annotation, leading questions, the illusion of emergent abilities, and, as it allows to use newly created images without annotation, training data contamination. Further, it is expected to result in slower benchmark saturation. Being adaptable to different modalities, the GenCception method can deliver value as a unified MLLM evaluation method that complements existing MLLM benchmarks.

Our empirical validation using the *MMEception* benchmark shows that GenCception effectively assesses semantic coherence and consistency across modalities, aligning with established VLLM benchmarks. By assessing humans on the *MMEception* task, we demonstrate that current VLLMs significantly lag behind human performance, particularly

when working with text-intensive images. Future work is encouraged to refine and extend this framework across a wider range of modalities, datasets, and similarity metrics.

References

- Achiam, J., Adler, S., Agarwal, S., Ahmad, L., Akkaya, I., Aleman, F.L., Almeida, D., Altenschmidt, J., Altman, S., Anadkat, S., et al., 2023. GPT-4 technical report. arXiv preprint arXiv:2303.08774 .
- Anthropic, 2023. Model card for claude. URL: https://www-cdn.anthropic.com/de8ba9b01c9ab7cbabf5c33b80b7bbc618857627/Model_Card_Claude_3.pdf. accessed: [13.05.2024].
- Chen, L., Li, J., Dong, X., Zhang, P., Zang, Y., Chen, Z., Duan, H., Wang, J., Qiao, Y., Lin, D., et al., 2024. Are we on the right way for evaluating large vision-language models? arXiv preprint arXiv:2403.20330 .
- Chen, X., Wu, Z., Liu, X., Pan, Z., Liu, W., Xie, Z., Yu, X., Ruan, C., 2025. Janus-Pro: Unified multimodal understanding and generation with data and model scaling. arXiv preprint arXiv:2501.17811.
- Coates, A., Ng, A., Lee, H., 2011. An analysis of single-layer networks in unsupervised feature learning, in: Proceedings of the fourteenth international conference on artificial intelligence and statistics, JMLR Workshop and Conference Proceedings. pp. 215–223.
- Dai, W., Li, J., Li, D., Tiong, A.M.H., Zhao, J., Wang, W., Li, B., Fung, P., Hoi, S., 2023. Instructblip: Towards general-purpose vision-language models with instruction tuning. arXiv preprint:2305.06500 .
- DeepMind, 2023. Imagegen2. <https://deepmind.google/technologies/imagegen-2/>. Accessed: [13.05.2024].
- Deng, J., Dong, W., Socher, R., Li, L.J., Li, K., Fei-Fei, L., 2009. ImageNet: A large-scale hierarchical image database, in: 2009 IEEE conference on computer vision and pattern recognition, pp. 248–255.
- Dodge, J., Sap, M., Marasović, A., Agnew, W., Ilharco, G., Groeneveld, D., Mitchell, M., Gardner, M., 2021. Documenting large webtext corpora: A case study on the colossal clean crawled corpus. arXiv preprint arXiv:2104.08758 .
- Dosovitskiy, A., Beyer, L., Kolesnikov, A., Weissenborn, D., Zhai, X., Unterthiner, T., Dehghani, M., Minderer, M., Heigold, G., Gelly, S., Uszkoreit, J., Housley, N., 2021. An image is worth 16x16 words: Transformers for image recognition at scale, in: International Conference on Learning Representations.
- Fu, C., Chen, P., Shen, Y., Qin, Y., Zhang, M., Lin, X., Yang, J., Zheng, X., Li, K., Sun, X., et al., 2023. MME: A comprehensive evaluation benchmark for multimodal large language models. arXiv preprint arXiv:2306.13394 .
- Heusel, M., Ramsauer, H., Unterthiner, T., Nessler, B., Hochreiter, S., 2017. Gans trained by a two time-scale update rule converge to a local nash equilibrium. Advances in neural information processing systems 30.
- Jiang, Y., Chan, C., Chen, M., Wang, W., 2023. Lion: Adversarial distillation of closed-source large language model. arXiv preprint arXiv:2305.12870 .
- Kemhavi, A., Salvato, M., Kolve, E., Seo, M., Hajishirzi, H., Farhadi, A., 2016. A diagram is worth a dozen images, in: Computer Vision–ECCV 2016: 14th European Conference, Amsterdam, The Netherlands, October 11–14, 2016, Proceedings, Part IV 14, Springer. pp. 235–251.
- Kiela, D., Bartolo, M., Nie, Y., Kaushik, D., Geiger, A., Wu, Z., Vidgen, B., Prasad, G., Singh, A., Ringshia, P., et al., 2021. Dynabench: Rethinking benchmarking in nlp, in: Proceedings of the 2021 Conference of the North American Chapter of the Association for Computational Linguistics: Human Language Technologies, pp. 4110–4124.
- Krizhevsky, A., Hinton, G., et al., 2009. Learning multiple layers of features from tiny images. Technical Report. Massachusetts Institute of Technology and New York University.
- Lee, Y., Park, I., Kang, M., 2024. FLEUR: An explainable reference-free evaluation metric for image captioning using a large multimodal model, in: Ku, L.W., Martins, A., Srikumar, V. (Eds.), Proceedings of the 62nd Annual Meeting of the Association for Computational Linguistics (Volume 1: Long Papers), Association for Computational Linguistics, Bangkok, Thailand. pp. 3732–3746. URL: <https://aclanthology.org/2024.acl-long>. doi:10.18653/v1/2024.acl-long.205.
- Li, B., Wang, R., Wang, G., Ge, Y., Ge, Y., Shan, Y., 2023a. Seed-bench: Benchmarking multimodal llms with generative comprehension. arXiv preprint arXiv:2307.16125 .
- Li, R., Patel, T., Du, X., 2023b. Prd: Peer rank and discussion improve large language model based evaluations. arXiv preprint arXiv:2307.02762 .
- Li, Y., Du, Y., Zhou, K., Wang, J., Zhao, W.X., Wen, J.R., 2023c. Evaluating object hallucination in large vision-language models. arXiv preprint:2305.10355 .
- Liu, F., Guan, T., Li, Z., Chen, L., Yacoob, Y., Manocha, D., Zhou, T., 2023a. Hallusionbench: You see what you think? or you think what you see? an image-context reasoning benchmark challenging for gpt-4v (ision), llava-1.5, and other multi-modality models. arXiv preprint arXiv:2310.14566 .
- Liu, H., Li, C., Li, Y., Lee, Y.J., 2023b. Improved baselines with visual instruction tuning, in: NeurIPS 2023 Workshop on Instruction Tuning and Instruction Following.
- Loya, M., Sinha, D.A., Futrell, R., 2023. Exploring the sensitivity of llms’ decision-making capabilities: Insights from prompt variation and hyperparameters. arXiv preprint arXiv:2312.17476 .
- OpenAI, 2024. Hello gpt-4o. OpenAI Technical Report Available at <https://openai.com/index/hello-gpt-4o/>.
- OpenCompass, 2023. OpenCompass: A universal evaluation platform for foundation models. <https://github.com/open-compass/opencompass>.
- Ramesh, A., Pavlov, M., Goh, G., Gray, S., Voss, C., Radford, A., Chen, M., Sutskever, I., 2021. Zero-shot text-to-image generation, in: International Conference on Machine Learning, PMLR. pp. 8821–8831.
- Reid, M., Savinov, N., Teplyashin, D., Lepikhin, D., Lillicrap, T., Alayrac, J.b., Soricut, R., Lazaridou, A., Firat, O., Schrittwieser, J., et al., 2024. Gemini 1.5: Unlocking multimodal understanding across millions of tokens of context. arXiv preprint arXiv:2403.05530 .
- Schaeffer, R., Miranda, B., Koyejo, S., 2023. Are emergent abilities of large language models a mirage? arXiv preprint arXiv:2304.15004 .
- Sun, G., Manakul, P., Liusie, A., Pipatanakul, K., Zhang, C., Woodland, P., Gales, M., 2024. Crosscheckgpt: Universal hallucination ranking for multimodal foundation models. arXiv preprint arXiv:2405.13684 .

- Wang, W., Chen, Z., Chen, X., Wu, J., Zhu, X., Zeng, G., Luo, P., Lu, T., Zhou, J., Qiao, Y., et al., 2023. Visionllm: Large language model is also an open-ended decoder for vision-centric tasks. arXiv preprint:2305.11175 .
- Wang, X., Zhang, X., Luo, Z., Sun, Q., Cui, Y., Wang, J., Zhang, F., Wang, Y., Li, Z., Yu, Q., et al., 2024. Emu3: Next-token prediction is all you need. arXiv preprint arXiv:2409.18869.
- Xie, J., Mao, W., Bai, Z., Zhang, D.J., Wang, W., Lin, K.Q., Gu, Y., Chen, Z., Yang, Z., Shou, M.Z., 2024. Show-o: One single transformer to unify multimodal understanding and generation. arXiv preprint arXiv:2408.12528.
- Xu, Z., Shen, Y., Huang, L., 2022. Multiinstruct: Improving multi-modal zero-shot learning via instruction tuning. arXiv preprint:2212.10773 .
- Yang, S., Chiang, W.L., Zheng, L., Gonzalez, J.E., Stoica, I., 2023. Rethinking benchmark and contamination for language models with rephrased samples. arXiv preprint arXiv:2311.04850 .
- Ye, Q., Xu, H., Ye, J., Yan, M., Liu, H., Qian, Q., Zhang, J., Huang, F., Zhou, J., 2023. mplug-owl2: Revolutionizing multi-modal large language model with modality collaboration. arXiv preprint:2311.04257 .
- Zhao, Y., Pang, T., Du, C., Yang, X., Li, C., Cheung, N.M., Lin, M., 2023. On evaluating adversarial robustness of large vision-language models. arXiv preprint:2305.16934 .

Appendix A. GenCepion Demonstration

To provide a comprehensive, intuitive and qualitative understanding of the GenCepion procedure and $GC@T$ metric, we illustrate the input, output, intermediate artifacts, similarity scores, and $GC@T$ values throughout the GenCepion process. Examples from the visual-intensive and textual-intensive groups are showcased in Figures B.5 and B.6, respectively. The corresponding seed images and their metadata are presented in Figure A.4.

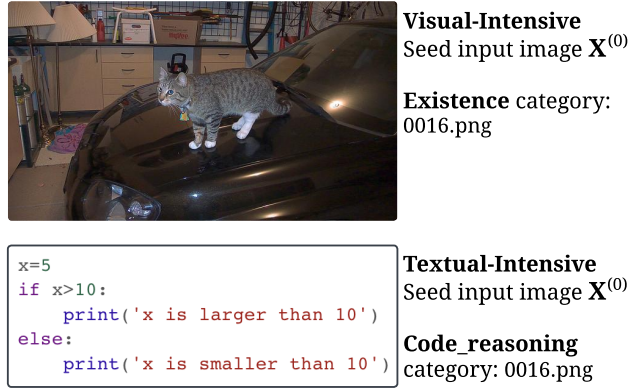


Figure A.4: Example seed images from the visually (Figure B.5) and textually (Figure B.6) intensive groups, along with their associated metadata.

Appendix B. Dataset and Reproducibility

In Sections 1, 2.1, 2.2 and 3 of the main paper, we cite the creators of all artifacts used. Detailed citations can be found in references. The MME dataset is not directly downloadable, and is released for research purposes only upon a request from authors to gain access to it. It does not contain any personally identifying information, as the questions regard visual aspects of the images. We followed the guidelines provided by the authors and respected the intended terms of use. The specific licenses and terms for the use and distribution of publicly available artifacts can be found in the corresponding original papers or GitHub repositories, as cited. As per this research work and aligning with the MME copyrights, we are not releasing this asset. Regarding the created artifacts, we introduce a new metric called $GC@T$, and detail its creation and intended use in Section 2.2 of the main paper. Our study exclusively utilizes images from the MME dataset, omitting textual QA annotations, and generates textual data in the form of English descriptions as part of our methodology. Given the nature of our research centered on quantifying the inter-modality coherence and consistency, we do not apply any data splits. Due to limitations in terms of computational resources, the metrics reported in Table 2 are from a single run.

In our study, we adopt several state-of-the-art models to facilitate our experiments, including Gemini1.5-Pro, GPT-4o, GPT-4V, Claude3-Opus, LLaVa-13B, LLaVa-7B, and mPLUG-Ow12 for text description generation, ViT for image embedding, and DALL-E 3 and Imagen2 for image generation, adhering to default parameter settings as

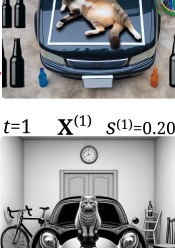
GPT-4o		<p>$t=1$ $X^{(1)}$ $s^{(1)}=0.29$</p> <p>$Q^{(1)}$ The image depicts a domestic scene inside a garage. The primary focus is a black cat sitting on a shelf, looking towards the camera. To the left of the cat, a white dog is visible, looking away. The background is filled with various tools, equipment, and items, suggesting a well-used workspace. The lighting is warm and focused on the cat, creating a cozy atmosphere. The overall scene is organized and tidy.</p>		<p>$t=2$ $X^{(2)}$ $s^{(2)}=0.31$</p> <p>$Q^{(2)}$ The image depicts a well-organized garage with various elements arranged. A black classic car is parked in the background. In the foreground, a black cat is sitting on a shelf, looking towards the camera. To the left of the cat, a white dog is visible, looking away. The background is filled with various tools, equipment, and items, suggesting a well-used workspace. The lighting is warm and focused on the cat, creating a cozy atmosphere. The overall scene is organized and tidy.</p>		<p>$t=3$ $X^{(3)}$ $s^{(3)}=0.23$</p> <p>$Q^{(3)}$ The image depicts a well-organized garage with a classic car, various tools, and other items. A black cat is sitting on a shelf, looking towards the camera. To the left of the cat, a white dog is visible, looking away. The background is filled with various tools, equipment, and items, suggesting a well-used workspace. The lighting is warm and focused on the cat, creating a cozy atmosphere. The overall scene is organized and tidy.</p>	GC@3 = 0.27
Gemini1.5-Pro		<p>$t=1$ $X^{(1)}$ $s^{(1)}=0.46$</p> <p>$Q^{(1)}$ A black cat with a white collar and a gold tag sits on the head of a black vintage car in a cluttered garage. The cat is looking towards the camera. The background is filled with various tools, equipment, and items, suggesting a well-used workspace. The lighting is warm and focused on the cat, creating a cozy atmosphere. The overall scene is organized and tidy.</p>		<p>$t=2$ $X^{(2)}$ $s^{(2)}=0.29$</p> <p>$Q^{(2)}$ The image depicts a well-organized garage with various elements arranged. A black classic car is parked in the background. In the foreground, a black cat is sitting on a shelf, looking towards the camera. To the left of the cat, a white dog is visible, looking away. The background is filled with various tools, equipment, and items, suggesting a well-used workspace. The lighting is warm and focused on the cat, creating a cozy atmosphere. The overall scene is organized and tidy.</p>		<p>$t=3$ $X^{(3)}$ $s^{(3)}=0.39$</p> <p>$Q^{(3)}$ A long-haired black cat with vibrant green eyes sits on the head of a black vintage car in a cluttered garage. The cat is looking towards the camera. The background is filled with various tools, equipment, and items, suggesting a well-used workspace. The lighting is warm and focused on the cat, creating a cozy atmosphere. The overall scene is organized and tidy.</p>	GC@3 = 0.37
Claude3-Opus		<p>$t=1$ $X^{(1)}$ $s^{(1)}=0.30$</p> <p>$Q^{(1)}$ The image depicts a black cat sitting on the head of a black vintage car in a cluttered garage. The cat is looking towards the camera. The background is filled with various tools, equipment, and items, suggesting a well-used workspace. The lighting is warm and focused on the cat, creating a cozy atmosphere. The overall scene is organized and tidy.</p>		<p>$t=2$ $X^{(2)}$ $s^{(2)}=0.33$</p> <p>$Q^{(2)}$ The image depicts a well-organized garage with various elements arranged. A black classic car is parked in the background. In the foreground, a black cat is sitting on a shelf, looking towards the camera. To the left of the cat, a white dog is visible, looking away. The background is filled with various tools, equipment, and items, suggesting a well-used workspace. The lighting is warm and focused on the cat, creating a cozy atmosphere. The overall scene is organized and tidy.</p>		<p>$t=3$ $X^{(3)}$ $s^{(3)}=0.33$</p> <p>$Q^{(3)}$ In the whimsical image, a black cat sits atop the hood of a vintage Chevrolet, its white paws gripping the edge. The cat's gaze is directed towards the viewer, its eyes reflecting the ambient light. The background is a cluttered garage, filled with various tools, equipment, and items, suggesting a well-used workspace. The lighting is warm and focused on the cat, creating a cozy atmosphere. The overall scene is organized and tidy.</p>	GC@3 = 0.33
GPT-4V		<p>$t=1$ $X^{(1)}$ $s^{(1)}=0.30$</p> <p>$Q^{(1)}$ The image depicts a domestic cat sitting on the head of a black vintage car in a cluttered garage. The cat is looking towards the camera. The background is filled with various tools, equipment, and items, suggesting a well-used workspace. The lighting is warm and focused on the cat, creating a cozy atmosphere. The overall scene is organized and tidy.</p>		<p>$t=2$ $X^{(2)}$ $s^{(2)}=0.33$</p> <p>$Q^{(2)}$ The image depicts a well-organized garage with various elements arranged. A black classic car is parked in the background. In the foreground, a black cat is sitting on a shelf, looking towards the camera. To the left of the cat, a white dog is visible, looking away. The background is filled with various tools, equipment, and items, suggesting a well-used workspace. The lighting is warm and focused on the cat, creating a cozy atmosphere. The overall scene is organized and tidy.</p>		<p>$t=3$ $X^{(3)}$ $s^{(3)}=0.24$</p> <p>$Q^{(3)}$ The image depicts a well-organized garage interior with a focus on a black cat sitting on the head of a vintage car. The cat is looking towards the camera. The background is filled with various tools, equipment, and items, suggesting a well-used workspace. The lighting is warm and focused on the cat, creating a cozy atmosphere. The overall scene is organized and tidy.</p>	GC@3 = 0.23
mPLUG-Owl2		<p>$t=1$ $X^{(1)}$ $s^{(1)}=0.33$</p> <p>$Q^{(1)}$ The image features a cat standing on the hood of a black car. The cat is positioned towards the center of the frame, looking towards the camera. The background is filled with various tools, equipment, and items, suggesting a well-used workspace. The lighting is warm and focused on the cat, creating a cozy atmosphere. The overall scene is organized and tidy.</p>		<p>$t=2$ $X^{(2)}$ $s^{(2)}=0.31$</p> <p>$Q^{(2)}$ The image depicts a well-organized garage with various elements arranged. A black classic car is parked in the background. In the foreground, a black cat is sitting on a shelf, looking towards the camera. To the left of the cat, a white dog is visible, looking away. The background is filled with various tools, equipment, and items, suggesting a well-used workspace. The lighting is warm and focused on the cat, creating a cozy atmosphere. The overall scene is organized and tidy.</p>		<p>$t=3$ $X^{(3)}$ $s^{(3)}=0.24$</p> <p>$Q^{(3)}$ The image features a large, modern, and luxurious BMW car parked in a garage. The car is positioned in the center of the frame, surrounded by various tools, equipment, and items. The lighting is warm and focused on the car, creating a cozy atmosphere. The overall scene is organized and tidy.</p>	GC@3 = 0.20
LLaVA-13B		<p>$t=1$ $X^{(1)}$ $s^{(1)}=0.18$</p> <p>$Q^{(1)}$ The image features a cat sitting on top of a car. The cat is positioned in the center of the frame, looking towards the camera. The background is filled with various tools, equipment, and items, suggesting a well-used workspace. The lighting is warm and focused on the cat, creating a cozy atmosphere. The overall scene is organized and tidy.</p>		<p>$t=2$ $X^{(2)}$ $s^{(2)}=0.44$</p> <p>$Q^{(2)}$ The image features a cat lying on the hood of a car. The cat is positioned in the center of the frame, looking towards the camera. The background is filled with various tools, equipment, and items, suggesting a well-used workspace. The lighting is warm and focused on the cat, creating a cozy atmosphere. The overall scene is organized and tidy.</p>		<p>$t=3$ $X^{(3)}$ $s^{(3)}=0.15$</p> <p>$Q^{(3)}$ The image depicts a room with a black sports car parked inside. The car is positioned in the center of the frame, surrounded by various tools, equipment, and items. The lighting is warm and focused on the car, creating a cozy atmosphere. The overall scene is organized and tidy.</p>	GC@3 = 0.17
LLaVA-7B		<p>$t=1$ $X^{(1)}$ $s^{(1)}=0.20$</p> <p>$Q^{(1)}$ The image features a black car with a cat sitting on its hood. The cat is positioned towards the center of the frame, looking towards the camera. The background is filled with various tools, equipment, and items, suggesting a well-used workspace. The lighting is warm and focused on the cat, creating a cozy atmosphere. The overall scene is organized and tidy.</p>		<p>$t=2$ $X^{(2)}$ $s^{(2)}=0.24$</p> <p>$Q^{(2)}$ The image features a black car parked in a room. The car is positioned in the center of the frame, surrounded by various tools, equipment, and items. The lighting is warm and focused on the car, creating a cozy atmosphere. The overall scene is organized and tidy.</p>		<p>$t=3$ $X^{(3)}$ $s^{(3)}=0.31$</p> <p>$Q^{(3)}$ The image depicts a room with a black sports car parked inside. The car is positioned in the center of the frame, surrounded by various tools, equipment, and items. The lighting is warm and focused on the car, creating a cozy atmosphere. The overall scene is organized and tidy.</p>	GC@3 = 0.23

Figure B.5: Illustration of a 3-iteration GenCepition procedure run on a **visual-intensive** image (from “existence” category) to evaluate 7 VLLMs. Each iteration t shows the generated image $X^{(t)}$, the description $Q^{(t)}$ of the preceding image $X^{(t-1)}$, and the similarity score $s^{(t)}$ relative to $X^{(0)}$. The GC@3 metric for each VLLM is also presented. Hallucinated elements within descriptions $Q^{(1)}$ and $Q^{(2)}$ as compared to the seed image are indicated with **red underlining**.



Figure B.6: Illustration of a 3-iteration GenCepTION procedure run on a **textual-intensive** image (from “code reasoning” category) to evaluate 7 VLLMs. Each iteration t shows the generated image $X^{(t)}$, the description $Q^{(t)}$ of the preceding image $X^{(t-1)}$, and the similarity score $s^{(t)}$ relative to $X^{(0)}$. The GC@3 metric for each VLLM is also presented. Hallucinated elements within descriptions $Q^{(1)}$ as compared to the seed image are indicated with **red underlining**.

outlined in their original specifications. As we only evaluated existing models but did not train new models, no hyperparameter tuning was applicable. The text descriptions generated by GPT-4V/4o, Claude3 and Gemini1.5 are obtained through API calls, while experiments involving the other models are conducted on A100 GPUs, totaling approximately 96 GPU hours. Image generation was also performed via a call to OpenAI’s DALL-E 3 API. To compute the $GC@T$ metric, we employ the cosine similarity metric from the Scikit-learn library (Version 1.4.0).

Appendix C. Human Annotators

As described in Section 3, we benchmarked the performance of humans at the $GC@T$ task. The 5 human annotators were recruited from the authors’ social circle and were being made aware that they contributed to a research project, with the specific goal of the research project only being disclosed after participation. They were provided with the same instruction prompt as the MLLMs, and given 14 weeks to complete the task. This task does not involve sharing any personal information and the images were carefully evaluated to not be offensive in any way. The participants gave consent that their annotations could be used for scientific research and included in research papers.

Appendix D. AI Assistants

AI assistants like GitHub Copilot, ChatGPT, and Perplexity were used to support writing the necessary codebase and find efficient ways to express complex concepts. AI assistant suggestions were always carefully evaluated for correctness and only used after human revision.